OPEN ACCESS
IOP PUBLISHING ENVIRONMENTAL RESEARCH LETTERS
Environ. Res. Lett. **7** (2012) 044039 (8pp) doi:10.1088/1748-9326/7/4/044039

The footprint of Alaskan tundra fires during the past half-century: implications for surface properties and radiative forcing

Adrian V Rocha[1,2,11], Michael M Loranty[3], Phil E Higuera[4], Michelle C Mack[5], Feng Sheng Hu[6], Benjamin M Jones[7], Amy L Breen[8], Edward B Rastetter[9], Scott J Goetz[10] and Gus R Shaver[9]

[1] Department of Biological Sciences, University of Notre Dame, Notre Dame, IN 46556, USA
[2] Environmental Change Initiative, University of Notre Dame, Notre Dame, IN 46556, USA
[3] Department of Geography, Colgate University, Hamilton, NY 13346, USA
[4] College of Natural Resources, University of Idaho, Moscow, ID 83844, USA
[5] Department of Biology, University of Florida, Gainesville, FL 32611, USA
[6] Department of Plant Biology, University of Illinois, Urbana, IL 61801, USA
[7] Alaska Science Center, US Geological Survey, 4210 University Drive, Anchorage, AK 99508, USA
[8] International Arctic Research Center, University of Alaska, Fairbanks, AK 99709, USA
[9] The Ecosystems Center, Marine Biological Laboratory, Woods Hole, MA 02543, USA
[10] Woods Hole Research Center, Falmouth, MA 02536, USA

E-mail: arocha1@nd.edu

Received 20 August 2012
Accepted for publication 29 November 2012
Published 19 December 2012
Online at stacks.iop.org/ERL/7/044039

Abstract
Recent large and frequent fires above the Alaskan arctic circle have forced a reassessment of the ecological and climatological importance of fire in arctic tundra ecosystems. Here we provide a general overview of the occurrence, distribution, and ecological and climate implications of Alaskan tundra fires over the past half-century using spatially explicit climate, fire, vegetation and remote sensing datasets for Alaska. Our analyses highlight the importance of vegetation biomass and environmental conditions in regulating tundra burning, and demonstrate that most tundra ecosystems are susceptible to burn, providing the environmental conditions are right. Over the past two decades, fire perimeters above the arctic circle have increased in size and importance, especially on the North Slope, indicating that future wildfire projections should account for fire regime changes in these regions. Remote sensing data and a literature review of thaw depths indicate that tundra fires have both positive and negative implications for climatic feedbacks including a decadal increase in albedo radiative forcing immediately after a fire, a stimulation of surface greenness and a persistent long-term (>10 year) increase in thaw depth. In order to address the future impact of tundra fires on climate, a better understanding of the control of tundra fire occurrence as well as the long-term impacts on ecosystem carbon cycling will be required.

Keywords: tundra, fire, radiative forcing, albedo, EVI, climate change

S Online supplementary data available from stacks.iop.org/ERL/7/044039/mmedia

[11] Address for correspondence: Department of Biological Sciences, University of Notre Dame, USA.

1. Introduction

Fires are an important driver of ecosystem change, global carbon cycling, and climate forcing, but are not evenly distributed across the globe (Bowman *et al* 2009). In Alaska, fires mostly occur in the interior boreal forests, and are less frequent in tundra (Kasischke and Turetsky 2006). Low aboveground biomass, ignition sources and temperatures have been thought to limit fire in tundra regions, and as a result, fire activity in these areas has been largely ignored in Alaskan and global fire simulations or assessments (Bond *et al* 2005, Bowman *et al* 2009, Krawchuk *et al* 2009). Although fire is considered rare in arctic tundra, it does occur. Historically, Alaskan tundra fires have been most frequent on the Seward Peninsula, but rare in other parts of Alaska, Canada, and Siberia (Wein 1976, Racine *et al* 1985). However, a large unprecedented fire on the North Slope in 2007 and a large number of fires in the Noatak in 2010 have forced a reassessment of the importance of tundra fires across the region (Jones *et al* 2009, Hu *et al* 2010, Higuera *et al* 2008). It remains to be determined if these changes to the arctic fire regime can be attributed to recent changes in climate (i.e. increased growing season, temperature, precipitation) (Hu *et al* 2010, Joly *et al* 2012). However, analyzing the spatial and temporal variability in tundra fire occurrence may reveal the sensitivity of fire in this ecosystem to current climate and thereby help in predicting fire regimes under future changes in climate.

Fires affect ecosystem properties and climate over a variety of spatial and temporal scales. Fires drastically alter the influence of arctic tundra on climate by charring the surface, which decreases albedo, and releasing a large amount of soil carbon stocks in the form of CO_2 to the atmosphere. Both of these changes result in a warming effect on the atmosphere (i.e. a positive radiative forcing) during and immediately after burning (Mack *et al* 2011, Rocha and Shaver 2011b), but the duration and impact of these changes remains poorly quantified. For example, fires also alter the microenvironment and increase soil temperatures, thaw depth and nutrient availability that may enhance plant productivity and soil respiration for several years after fire (Fetcher *et al* 1984, Wein and Bliss 1973, Vavrek *et al* 1999). Consequently, the long-term impact of tundra fires consists of many, offsetting or enhancing, feedbacks on climate that will depend on the rate and ability of the surface and subsurface properties to recover after fire.

We analyzed moderate resolution imaging spectroradiometer (MODIS) remote sensing data, field and literature survey of thaw depth measurements, and climate data to better understand tundra fire regimes and their long-term (i.e. multi-decadal) impacts on surface properties across Alaskan tundra. The data set included a vegetation map, a 61 year record of the spatial and temporal extent of tundra fires, and a spatially explicit climate record for Alaska. Data were combined with MODIS enhanced vegetation index (EVI; surface greenness) and albedo from 2001–11 to address the following questions:

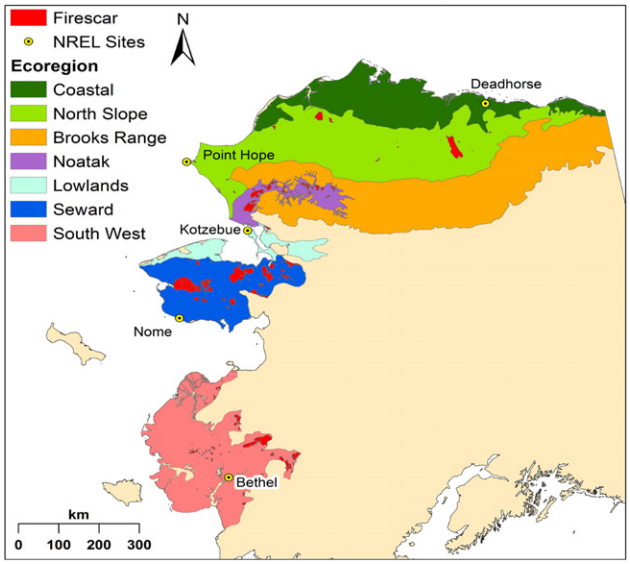

Figure 1. Map of tundra ecoregions, NREL sites and tundra fire scar distributions in Alaska.

- How has the spatial extent of fires varied across Alaskan tundra regions over the past 61 years?
- How do surface properties, such as surface greenness, albedo, albedo radiative forcing and thaw depth change after fire?

Addressing these questions provides critical information for understanding the potential impacts of a changing fire regime on land surface properties in arctic tundra.

2. Data and methods

2.1. Vegetation cover and fire history

Spatial data from a variety of sources were used to examine the spatial and temporal distribution of fire in Alaskan tundra. Tundra ecological regions were defined by the 2001 unified ecoregions map of Alaska (http://agdc.usgs.gov/), that combines the Bailey and Omernik approach to ecoregion mapping (Nowacki *et al* 2001). The map was slightly modified to delineate the Noatak watershed as a separate ecoregion from the North Slope and Mountain ecoregions, as the Noatak watershed differs substantially in its elevation, vegetation cover and climate than the rest of these ecoregions (see figure 1). Tundra vegetation was delineated using the Alaskan arctic tundra vegetation map, which includes the spatial distribution of 85 plant community descriptions across Alaska at a spatial resolution of ∼14 km (Raynolds *et al* 2006). The historical fires database from the Alaskan Interagency Coordination Center (http://fire.ak.blm.gov) was used to identify the year, area and location of fires from 1950 to 2011. Fire perimeters were mapped using a variety of methods including helicopter and ground surveys conducted by the Bureau of Land Management. The uncertainty of the fire locations varies from 200 to 500 m, depending on the location

and time of the fire (i.e. remote and older fire perimeters contain more uncertainty) (Kasischke and Turetsky 2006). Each fire perimeter was separated into areas that burned once and repeatedly during the 1950–2011 period.

Analysis was restricted to Alaskan tundra ecoregions with a historical fire record (figure 1). We estimated the fire rotation period (FRP) in each ecoregion using equation (1):

$$\mathrm{FRP} = \frac{t}{\sum_{i=1}^{n} a_i/A} \quad (1)$$

where t is the total length of the fire record (i.e. 2011–1950 = 61 yr), A is the size of the ecoregion, and a_i is the area (km^2) of each individual fire perimeter within the ecoregion (Baker 2009). The FRP is equal to the fire cycle and is the inverse of the mean fire return interval (i.e. the average number of years between consecutive fires at a point on the landscape). The mean fire interval (MFI) was estimated as the average time between any two consecutive burns in one location in space. The MFI provides a point-based estimate of fire occurrence, whereas the FRP provides an area-based estimate of fire occurrence. MFI provided a lower limit on fire frequency, whereas FRP provided an average fire frequency for a specific ecoregion. Area burned for each decade and ecoregion was calculated and ranked among the ecoregions in order of largest (i.e. 1) to smallest (i.e. 4).

Per cent area for each major vegetation type within each ecoregion and within each burn was calculated with the vegetation and fire history datasets. Vegetation units were aggregated into seven ecologically coherent vegetation types that consisted of moist shrub tundra (Vegetation units: S1.1, S1.2, S1.3, S1.4, S2.1, S2.2), moist tussock (i.e. acidic) tundra (G4.1, G4.2, G4.3), moist non-acidic tundra (G3.1, G3.3), wet shrub tundra (W3.2, W3.3, W3.4), wet tussock (i.e. acidic) tundra (W3.1), wet non-acidic tundra (W2.1, W2.2, W3.6) and barrens (B2.1, B3e.1, B3e.2, B4d.1, B4e.1, B4e.2). A Chi-squared test determined whether fires were randomly distributed across tundra ecoregions or predominant in some vegetation units compared to others. The proportion of each ecosystem burned (i.e. observed) was compared to the expected proportion of ecosystem burned under the null hypothesis of equal burning among ecoregions (i.e. expected). Significance was determined at the 90% confidence level.

2.2. Climate data

Parameter-elevation Regressions on Independent Slopes Model (PRISM; Daly *et al* 2000) data were used to determine climatological differences among ecoregions. PRISM uses point measurements of precipitation, temperature, and digital elevation models to produce continuous, digital grid estimates of monthly climate (1971–2000) averages of temperature and total precipitation at 400 m resolution. We also obtained National Renewable Energy Laboratory (NREL: www.nrel.gov) 1991–2005 monthly averaged diffuse, direct and global solar radiation data from sites located within each ecoregion (see figure 1 for site locations). Solar radiation data from the Bethel airport was used for the Southwest ecoregion, the Nome municipal airport was used for the Seward ecoregion, the Kotzebue airport was used for the Noatak ecoregion, and the average of the Deadhorse and Point Hope sites were used for the North Slope ecoregion.

2.3. MODIS albedo, surface temperature and vegetation indices

MODIS data products were used to characterize albedo, land surface temperature (LST) and the enhanced vegetation index (EVI) throughout the study ecoregions from 2001–11. The MCD43A3 nadir reflectance product, derived using Bidirectional Reflectance Distribution Functions (BRDF: Schaaf *et al* 2002) was used to map direct and diffuse broadband albedo (0.3–5.0 mm) at 500 m resolution. Data were screened using the associated quality control flags so that only the highest quality pixels (i.e. full BRDF inversion) with solar zenith angles less than 70° were retained for analysis (Liu *et al* 2009). Actual albedo (blue sky) was calculated as the average of direct and diffuse albedo weighted by the proportions of direct and diffuse global radiation from NREL data. The MOD13A1 product was used to map EVI at 500 m resolution, and data were screened to retain only good quality pixels (Huete *et al* 2002). Surface temperature, calculated as the mean of daytime and nighttime LST values, was mapped at 1 km resolution using the MOD11A2 product after screening to include only good quality data according to the embedded QA flags (Wan *et al* 2002). The MOD13A1 and MCD43A3 products represent mean values collected over a 16 day compositing period, with overlapping compositing periods produced every 8 days. The MOD11A2 LST products represent 8 day means with non-overlapping compositing periods.

2.4. Thaw depth

A literature search was conducted on thaw depth measurements for tundra fire scars of different age. Thaw depth is a measure of the seasonally unfrozen portion of the soil column (i.e. the active layer) that lies atop perennially frozen ground (i.e. permafrost). A total of nine studies were found through the ISI Web of Science that reported fire age and thaw depths inside both a fire scar and a nearby control. We also report the average of 30 unpublished thaw depth measurements obtained in random points within the Kuparuk 2001 fire scar (69.038N, −149.513W) on 27 July 2011 by the main author. Evidence of fire at this site was noted by the presence of dead and charred tussocks. Thaw depth measurements from the unburned Anaktuvuk River fire site, ∼30 km to the west, taken on the same day were used as a reference for the Kuparuk 2001 fire scar (Rocha and Shaver 2011a). Thaw depth data from the Anaktuvuk River fire mesonet from Rocha and Shaver (2011b) for the month of July were used for this analysis.

2.5. Energy balance and potential evapotranspiration

PRISM data, MODIS albedo and MODIS average surface temperature were used to calculate the monthly climate moisture index (CMI). The CMI is a measure of surface water balance and was calculated as the difference between monthly

Table 1. Climate and fire statistics.

	North slope	Noatak	Seward	Southwest
Variable	Climate Statistics			
Average air T (°C)[a]	8.6	10.5	9.9	11.2
Annual PPT (cm)[b]	16.6	21.9	19.6	45.7
Climate moisture index (CMI) (cm)[a]	−2.1	−7.1	−3.6	−2.5
	Ecoregion and fire statistics			
Ecoregion area (km^2)	115 221	15 049	47 307	76 623
Total area burned (km^2)	1606	2155	6800	2469
Reburned area (km^2)	0	367	1904	123
Number of fires	40	156	174	173
Max. reburns	1	3	4	2
Mean fire interval (MFI)	NA	13	18	22
61 year fire rotation period (FRP)	4374	425	424	1893

[a] June–August average.

[b] Annual sum.

precipitation (PPT) and Potential EvapoTranspiration (PET) (i.e. CMI = PPT − PET). Hence, a negative CMI indicates dry surface conditions, and a positive CMI indicates wet surface conditions. PET was calculated for each month and ecoregion using the Priestley–Taylor method with an alpha of 1.26 (Hogg 1997), PRISM monthly air temperature, and the balance between net short- (SW_b) and long-wave (LW_b) radiation (i.e. net radiation = SW_b+LW_b). Monthly incoming short-wave radiation from NREL (SW_i) and MODIS albedo (α) derived the short-wave balance ($SW_b = SW_i(1 - \alpha)$), while the Stefan–Boltzmann equation with an emissivity (ε_a) of 0.7 for PRISM air temperature (T_a), and an emissivity of 0.97 (ε_s) for MODIS surface temperature (T_s) derived the long-wave balance ($LW_b = 5.67 \times 10^{-5}$ ($\varepsilon_a T_a^4 - \varepsilon_s T_s^4$)) of net radiation.

2.6. Post-fire trajectories

A chronosequence approach utilizing time since fire for each fire perimeter was used to determine post-fire trajectories of MODIS surface EVI, albedo, annual albedo radiative forcing and thaw depth. Trajectories for each variable were determined by subtracting values within each fire perimeter for each year's growing season (i.e. May–September) with an unburned reference (Δ = burned − unburned). The unburned reference for the remote sensing data was calculated for each ecoregion as the 10 year average of all unburned tundra areas within the ecoregion. A positive Δ indicated that the particular variable increased after fire, while a negative Δ indicated that the particular variable decreased after fire. Given the spatial resolution of the MODIS data and the small number of old (i.e. >40 yr) and repeatedly burned fire perimeters, we only analyzed fire perimeters that burned once, were larger than 8 km^2, and were less than 40 years of age.

Radiative forcing (RF) was calculated for each month following equation (2) (Jin and Roy 2005):

$$RF = -\Delta\alpha SW_i \quad (2)$$

where $\Delta\alpha$ represents the monthly change in albedo, and SW_i represents the monthly averaged incoming global solar radiation from NREL for each ecoregion. Annual radiative forcing was calculated as the 12-month average of RF. By definition, a positive RF has a warming effect on climate, whereas a negative RF has a cooling effect on climate (IPCC 2007). Δ EVI, $\Delta\alpha$ and RF values were then averaged based on time since fire for each ecoregion and averaged among ecoregions to develop a single post-fire trajectory for each variable. 90% confidence intervals were constructed from the variability around the mean of the four trajectories using a Student t-distribution. In all, post-fire trajectories consisted of data from 108 fire perimeters; 7 from North Slope, 35 from Noatak, 33 from Seward and 33 from Southwest ecoregions.

3. Results

3.1. Spatial and temporal patterns of burned area

Wildfires occurred in four of the seven tundra ecoregions; the North Slope, Noatak, Seward and Southwest, which differed substantially in their climate and Fire Rotation Period (FRP) (figure 1; table 1). Growing season air temperature and annual precipitation were highest within the Southwest and lowest within the North Slope ecoregion. Differences in air temperature and precipitation had offsetting impacts on the available moisture as measured by the climate moisture index (CMI). Growing season CMI was high within the North Slope and Southwest, and low within the Seward and Noatak ecoregions. Ecoregions with low CMI (i.e. Noatak and Seward ecoregions) were associated with a large amount of total burned area. Of the total area burned, 0% was burned more than once in the North Slope, 17% was burned more than once in the Noatak, 28% was burned more than once in the Seward, and 5% was burned more than once in the Southwest. For sites that burned more than once, the average interval between fires (i.e. MFI) was 13 years for the Noatak, 18 years for the Seward and 22 years for the Southwest ecoregions. FRP for the 61 year record ranged from ∼400 years in the Noatak and Seward to thousands of years for the North Slope and Southwest ecoregions.

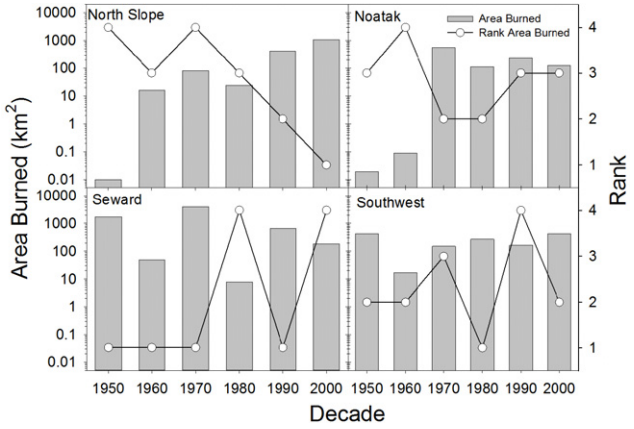

Figure 2. Decadal fire history in the four ecoregions; the North Slope, Noatak, Seward and Southwest. The left hand axis is on a common log scale and is associated with decadal area burned (gray bars), while the right hand axis is associated with the area burned ranking among the four ecoregions (open circles).

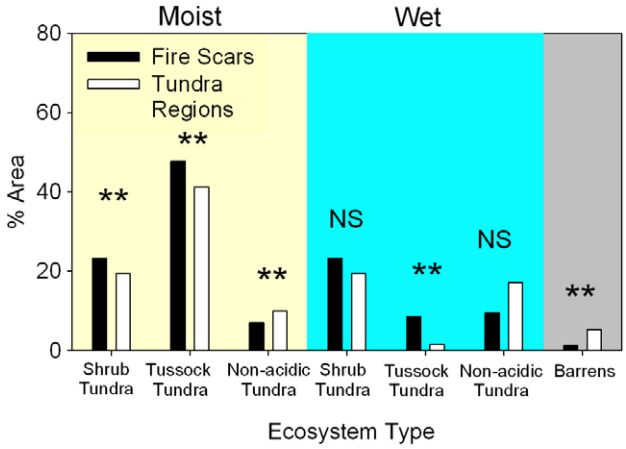

Figure 3. Per cent area of different ecosystem types in tundra ecoregions (white bars) and burned areas (black bars). Stars indicate statistical significance with Chi-squared test, and NS indicates not statistically significant at the 90% confidence level.

Area burned per decade and ecoregion burned area rankings varied among ecoregions and over time (figure 2). Decadal area burned spanned several orders of magnitude and were plotted on a log scale to compare their relative magnitudes across space and time. In the two more northern ecoregions that are above the arctic circle, decadal area burned exhibited large increases in the North Slope and Noatak from the 1950s to 2000s. The North Slope ecoregion ranked either the third or fourth largest decadal area burned among the four ecoregions in the 1950s and 1960s, but dramatically decreased in ranking to the second largest area burned in the 1990s, and the largest area burned in the 2000s among all of the ecoregions. Decadal area burned exhibited no clear temporal trends in the two southern ecoregions. The Seward had the largest decadal area burned among the four ecoregions from the 1950s to 1970s and in the 1990s, but the fourth largest decadal area burned in the 1980s and 2000s. Average area burned over the 61 years was 971 km^2 for the Seward, and 352 km^2 for the Southwest ecoregion. Decadal area burned from the North Slope ecoregion reached similar magnitude to that observed in the more fire active Seward ecoregion during the past two decades with an average 1990–2000s decadal area burned of 744 km^2.

Fires burned more area in some vegetation types than in others (figure 3). Within the ecoregions, moist tussock tundra was the most common, while wet tussock tundra was the least common vegetation type. Within fire perimeters, moist tundra types accounted for more total burned area than wet tundra types. Some vegetation types had more area burned than expected (χ^2: 64.3; d.f.:1; p-value < 0.001), indicating that burning was biased towards some vegetation types (i.e. shrub and tussock tundra) than others (i.e. non-acidic and Barrens). For example, moist tussock tundra covered 41% of the Alaskan tundra region, but contributed 47% of the area burned. Barrens, by contrast, covered 5% of the region, but contributed 1% of the burned area. Moist shrub, moist tussock, and wet tussock had significantly greater representation on an area basis within fire perimeters than observed across the landscape. Moist non-acidic and barrens had significantly smaller representation on an area basis within fire perimeters than observed across the landscape.

3.2. Post-fire effects on surface properties and thaw depth

Integrated analyses across tundra regions showed that remotely sensed surface properties recovered within a decade after fire (figure 4). There did not appear to be a difference in remotely sensed surface property trajectories among ecoregions, but comparisons were limited because of low sample size (supplementary figure available at stacks.iop.org/ERL/7/044039/mmedia). Trajectories had a larger representation of very young (i.e. <5 yr) and older (i.e. >25 yr) aged sites because of the greater availability of large (>8 km^2) tundra fire perimeters in these age classes. Post-fire EVI was lowest right after fire, increased to pre-fire levels within a decade, and was slightly higher than unburned tundra from 10 to 40 years after fire (figure 4(A)). Albedo followed a similar trajectory, recovering within 10 years, and highest 30–40 years after fire (figure 4(C)). Annual radiative forcing due to albedo peaked immediately after fire at 2.0 W m^{-2}, and decreased by 0.18 W m^{-2} yr^{-1} to zero 9 years after fire (figure 4(D)). Average albedo radiative forcing was 0.62 W m^{-2} over the first post-fire decade, and zero after a 40 year period.

Fire increased thaw depth in 75% of all reported burned areas (figure 5). Thaw depths were deeper than in unburned areas 24 year after fire. A majority of the shallower post-fire thaw depths were reported in Liljedahl *et al* (2007), whom expressed caution in comparing burned and unburned thaw depths because of rocky soils at their sites. Overall, thaw depths were significantly increased by 12% (T-test: 5.6, d.f.: 29; p-value < 0.001), and young (i.e. <10 yr) and old (i.e. >10 yr) burned sites were statistically indistinguishable (T-test: 0.18; d.f.: 29; p-value: 0.85). Fires increased thaw depth by 16% across all sites and ages when the sites of Liljedahl *et al* (2007) were excluded.

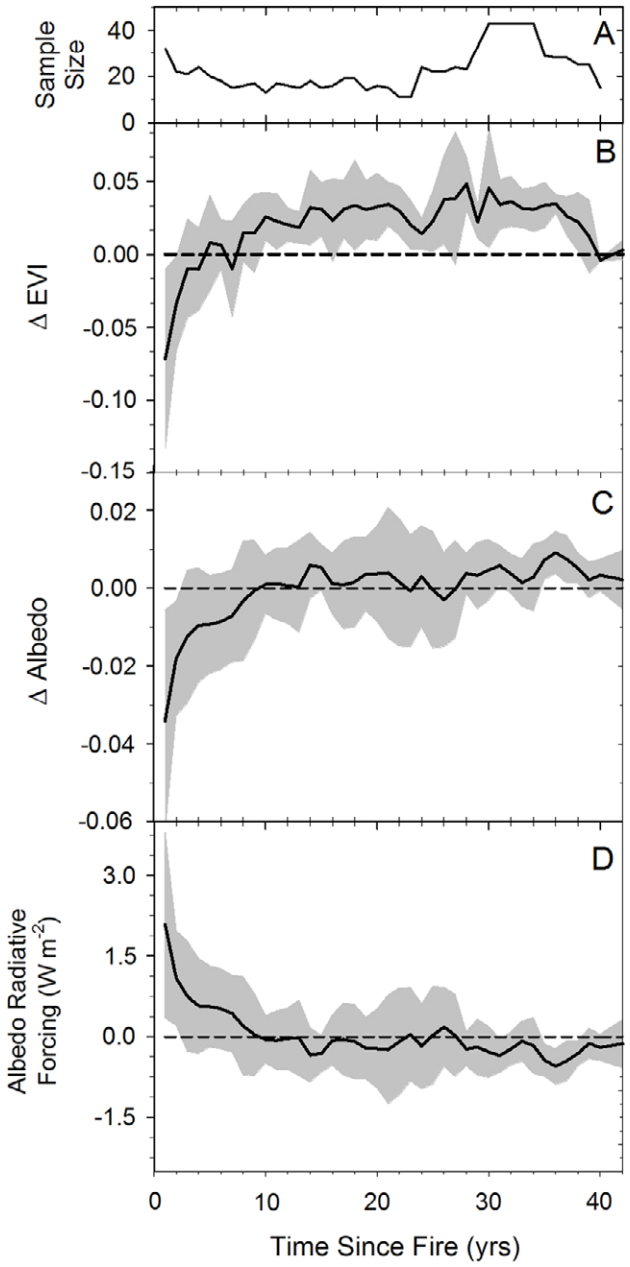

Figure 4. Post-fire trajectories of EVI (B), albedo (C) and albedo radiative forcing (D) in Alaskan tundra. Panel (A) illustrates the sample size for each variable as a function of time since fire. In panels (B)–(D), positive values indicated that the particular variable increased after fire, while negative values indicated that the particular variable decreased after fire. The hatched line indicates no change in the particular variable. The solid line in panels (B)–(D) is the average value of the four ecoregions, while the gray area indicates the 90% confidence interval.

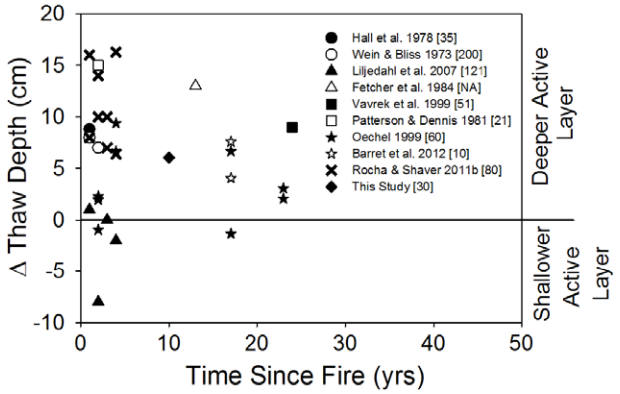

Figure 5. Post-fire changes in thaw depth obtained from the literature. Reported sample size for each burned/unburned pair reported in brackets following the citation. Positive values indicate greater thaw depth and a deeper active layer, while negative values indicate shallower thaw depth and active layer in fire scars of a given age.

4. Discussion

4.1. How has the spatial extent fires varied across the Alaskan tundra regions over the past 61 years?

Our results demonstrate that both environmental and biophysical factors influence tundra fire occurrence. It is clear through the analysis of the environmental conditions of the four ecoregions that tundra burning depends on more than one environmental factor (i.e. temperature or precipitation; Hu *et al* 2010). For example, the Southwest ecoregion had the highest growing season temperature and the third largest burned area, whereas the Seward ecoregion had the third highest temperature and the largest burned area among the four ecoregions. Regions with low available moisture (i.e. low CMI), which is a combination of both precipitation and temperature, had more frequent fires than regions with higher CMI, indicating the importance of surface water balance in regulating tundra fires (table 1) (also see Hu *et al* 2010). In addition, drier ecosystem types (i.e. moist) had greater percentage of their area burned than wetter (i.e. wet) ecosystem types (figure 3). These large scale patterns are consistent with tundra fire occurrences observed at the watershed scale, where fire rotation periods (Racine *et al* 1985), or mean fire return intervals are lower in areas with higher potential evapotranspiration rates (Higuera *et al* 2011). The larger representation of high aboveground biomass vegetation types (i.e. shrub and tussock tundra) within fire perimeters relative to their representation on the landscape also indicated the importance of fuel load and type in regulating tundra burning (figure 3) (Hu *et al* 2010, Higuera *et al* 2008, 2011). Low aboveground vegetation and moss biomass, a major source of fuel for tundra fires (Mack *et al* 2011), likely limit burned area in moist non-acidic and barren tundra. Vegetation productivity and surface dryness are expected to increase in the arctic over the next hundred years (ACIA 2004, Joly *et al* 2012), and if these large scale spatial patterns are indicative of the controls on tundra fire occurrence, then fire frequency and burned area in tundra will also increase in the future.

Detecting spatial and temporal trends of fire in infrequently burned areas is difficult over short time periods and with current fire records. Fire records prior to the 1970s are likely incomplete, due to observation limitations in remote areas (Kasischke and Turetsky 2006), and the inherent rarity of fires in the region complicate the detection of temporal trends. Despite these limitations, the dataset highlights several

new insights on the temporal and spatial dynamics of tundra fires over the past half-century. First, tundra fires are not as restricted to certain areas as previously thought (Racine *et al* 1985) with a majority of fires burning new territory during the past 61 years (table 1). Second, area burned above the arctic circle can be as large as that observed in more fire prone areas further south (i.e. Seward), and has increased in importance among the ecoregions with time, especially on the North Slope (figure 2). These observations point to a possible northern migration of fire and indicate that a majority of tundra regions are prone to burn providing the right environmental conditions (Higuera *et al* 2008, 2011). Our analyses also clearly demonstrate that fires above the arctic circle do occur and should be taken into account in future wildfire projections.

4.2. How do surface properties, such as surface greenness, albedo, albedo radiative forcing and thaw depth change after fire?

Despite the relative rarity of tundra fires during the past half-century, tundra surface properties (i.e. EVI and albedo) appear to recover rapidly after fire. Albedo and surface greenness dramatically declined immediately after fire, as a result of surface char and low vegetation cover, but recovered within a decade. The rapid recovery of vegetation cover after fire is likely due to the use of belowground carbon and nutrient reserves in the roots and rhizomes of tussock sedges (*Eriophorum vaginatum*) that are somewhat protected during combustion (Wein and Bliss 1973). Surface greenness was slightly elevated in fire perimeters after the second through fourth post-fire decade likely as a result of increased productivity and vegetation cover from either rapid recovery, or shifts in vegetation community composition (Wein and Bliss 1973, Racine *et al* 2004, Barrett *et al* 2012) (figure 5). Post-fire vegetation recovery can follow several trajectories with shifts from high albedo and low EVI tussock tundra to: low albedo and high EVI tall shrub tundra (Racine *et al* 2004), or high albedo and high EVI graminoid/low shrub dominated tundra (Rupp *et al* 2000). Since increased cover of tall shrubs should increase EVI and decrease albedo, the increase in greenness with very little change in albedo a decade after fire supports increased cover of graminoid species, or low stature shrubs, rather than a shift to tall shrub species with low albedo from 10 to 40 years after fire on average (figure 4). This does not indicate that all tundra will follow this post-fire trajectory, but represents an average post-fire trajectory from all tundra fires in the past 61 years. Burn severity, site history, and other environmental factors contribute variability to this mean response, but their effect on post-fire succession is poorly understood in tundra (but see Rocha and Shaver 2011a, 2011b).

Post-fire effects also had other long-term impacts on ecosystem function that could positively feedback on climate. Over the short term, tundra fires exerted a positive forcing (i.e. warming) on climate as carbon is released to the atmosphere during combustion, and albedo is reduced during the early stages of succession (figure 4). The decrease in albedo resulted in a strong positive radiative forcing immediately after fire, but this forcing only persisted for a decade and was essentially unimportant at multi-decadal timescales. Over the long term, deeper thaw depths in burned areas (figure 5) indicate warmer soils that can cause greater soil carbon decomposition, thermal erosion of permafrost, and even surface subsidence or thermokarst, which may result in greater emission of CO_2 into the atmosphere. Deeper thaw depths are likely due to combustion loss and slow recovery of mosses and the upper soil organic horizon, which play a large role in soil insulation and ground heat flux in tundra systems (Rocha and Shaver 2011b). The rapid recovery of vegetation cover also has implications for future fire regimes and climate change. Models predict that fire will convert the tundra to a graminoid/grassland dominated landscape that is more prone to reburn (Rupp *et al* 2000). Reburning of some sites within as little as 10–20 years in the Seward and Noatak ecoregions, and the increase in EVI from 20 to 40 years after fire appear to support these predictions (figure 4). Consequently, the complex balance of carbon cycling, fire frequency, and fire rotation periods over the long term will ultimately determine the net effect of tundra fires on climate.

5. Conclusions

Our analysis provides a general overview of the occurrence, distribution, and the ecological and climate implications of Alaskan tundra fires over the past half-century. We demonstrate that fire occurrence has varied over time and space (figures 1 and 2; table 1), that a majority of tundra ecosystems are prone to burn given the right environmental conditions (figure 3), that certain ecosystem types have been affected by fire more than others (figure 3), and that fires have both short- and long-term impacts on ecosystem properties (figures 4 and 5). Large uncertainties remain in determining the future arctic regime as well as the ecological and climate implications of these changes. These uncertainties include: how ignition sources (i.e. such as lightning and human activity) will change with climate, if future climate will drive tundra fires further north or into Canadian or Siberian tundra regions, how post-fire succession is affected by site history, burn severity, and other environmental factors, and what will be the long-term post-fire balance of plant productivity versus heterotrophic respiration. All of these issues are poorly understood and cannot be addressed with current data, but are critical in determining the future impact of the arctic on climate.

Acknowledgments

We thank Yueyang Jiang and three anonymous reviewers for comments on earlier drafts of this manuscript. This work was supported by NSF grants #1065587 to the Marine Biological Laboratory, Woods Hole. Any use of trade, product, or firm names is for descriptive purposes only and does not imply endorsement by the US Government.

References

ACIA 2004 *Impacts of a Warming Arctic: Arctic Climate Impact Assessment* (Cambridge: Cambridge University Press)

Baker W L 2009 *Fire Ecology in Rocky Mountain Landscapes* (Washington, DC: Island)

Barrett K *et al* 2012 Vegetation shifts observed in arctic tundra 17 yr after fire *Remote Sens. Lett.* **3** 729–36

Bond W J *et al* 2005 The global distribution of ecosystems in a world without fire *New Phytol.* **165** 525–38

Bowman D M J S *et al* 2009 Fire in the Earth system *Science* **324** 481–4

Daly C *et al* 2000 High quality spatial climate data sets for the United States and beyond *Trans. Am. Soc. Agricult. Eng.* **43** 1957–62

Fetcher N *et al* 1984 Changes in arctic tussock tundra thirteen years after fire *Ecology* **65** 1332–3

Hall D K *et al* 1978 The 1977 tundra fire in the Kokolik river area of Alaska *Arctic* **31** 54–8

Higuera P E *et al* 2008 Frequent fires in ancient shrub tundra: implications of paleorecords for arctic environmental change *PloS ONE* **3** e0001744

Higuera P E *et al* 2011 Variability of tundra fire regimes in Arctic Alaska: millennial-scale patterns and ecological implications *Ecol. Appl.* **21** 3211–26

Hogg E H 1997 Temporal scaling of moisture and the forest-grassland boundary in western Canada *Agricult. Forest Meteorol.* **84** 115–22

Hu F S *et al* 2010 Tundra burning in Alaska: linkages to climatic change and sea ice retreat *J. Geophys. Res.—Biogeosci.* **115** G04002

Huete A *et al* 2002 Overview of the radiometric and biophysical performance of the MODIS vegetation indices *Remote Sensing Environ.* **83** 195–213

IPCC 2007 *Climate Change 2007: The Physical Science Basis. Contribution of Working Group I to the Fourth Assessment Report of the Intergovernmental Panel on Climate Change* (Cambridge: Cambridge University Press)

Jin Y and Roy D P 2005 Fire-induced albedo change and its radiative forcing at the surface in northern Australia *Geophys. Res. Lett.* **32** L13401

Joly K *et al* 2012 Simulating the effects of climate change on fire regimes in arctic biomes: implications for caribou and moose habitat *Ecosphere* **3** 36

Jones B M *et al* 2009 Fire behavior, weather, and burn severity of the 2007 Anaktuvuk River tundra fire, North Slope, Alaska *Arct. Antarct. Alp. Res.* **41** 309–16

Kasischke E S and Turetsky M R 2006 Recent changes in the fire regime across the North American boreal region-spatial and temporal patterns of burning across Canada and Alaska *Geophys. Res. Lett.* **33** L09703

Krawchuk M A *et al* 2009 Global Pyrogeography: the current and future distribution of wildfire *PloS ONE* **4** e5102

Liljedahl A *et al* 2007 Physical short-term changes after a tussock tundra fire, Seward Peninsula, Alaska *J. Geophys. Res.—Earth Surf.* **112** F02S07

Liu J *et al* 2009 Validation of moderate resolution imaging spectroradiometer (MODIS) albedo retrieval algorithm: dependence of albedo on solar zenith angle *J. Geophys. Res.* **114** D01106

Mack M C *et al* 2011 Carbon loss from an unprecedented arctic tundra wildfire *Nature* **475** 489–92

Nowacki G *et al* 2001 Ecoregions of Alaska: 2001 *U.S. Geological Survey Open-File Report 02-297*

Oechel W C 1999 Net ecosystem carbon flux of age-specific subarctic tussock tundra stands following fire: implications for Alaska interagency fire management *Final Report to the National Park Service*

Patterson W A and Dennis J G 1981 Tussock replacement as a means of stabilizing fire breaks in tundra vegetation *Arctic* **34** 188–9

Racine C H *et al* 1985 Tundra fire regimes in the Noatak River Watershed Alaska: 1956–83 *Arct. Antarct. Alp. Res.* **19** 461–9

Racine C H *et al* 2004 Tundra fire and vegetation change along a hillslope on the Seward Peninsula, Alaska, USA *Arct. Antarct. Alp. Res.* **36** 1–10

Raynolds M K *et al* 2006 Alaska arctic tundra vegetation map 1:4,000,000 (Anchorage, AK: US Fish and Wildlife Service)

Rocha A V and Shaver G R 2011a Burn severity influences postfire CO_2 exchange in arctic tundra *Ecol. Appl.* **21** 477–89

Rocha A V and Shaver G R 2011b Post-fire energy exchange in arctic tundra: the importance and climatic implications of burn severity *Glob. Change Biol.* **17** 2831–41

Rupp T S *et al* 2000 A frame-based spatially explicit model of subarctic vegetation response to climate change: comparison with a point model *Landscape Ecol.* **15** 383–400

Schaaf C *et al* 2002 First operational BRDF, albedo and nadir reflectance products from MODIS *Remote Sensing Environ.* **83** 135–48

Wan Z *et al* 2002 Validation of the land-surface temperature products retrieved from Terra moderate resolution imaging spectroradiometer data *Remote Sens. Environ.* **83** 163–80

Wein R W 1976 Frequency and characteristics of arctic tundra fires *Arctic* **29** 213–22

Wein R W and Bliss L C 1973 Changes in arctic eriophorum tussock communities following fire *Ecology* **54** 845–52

Vavrek M C *et al* 1999 Recovery of productivity and species diversity in tussock tundra following disturbance *Arct. Antarct. Alp. Res.* **3** 291–304